Draft version October 2, 2018
Typeset using LaTeX **preprint** style in AASTeX62

A New High Perihelion Inner Oort Cloud Object

Scott S. Sheppard,[1] Chadwick A. Trujillo,[2] David J. Tholen,[3] and Nathan Kaib[4]

[1]*Department of Terrestrial Magnetism, Carnegie Institution for Science, 5241 Broad Branch Rd. NW, Washington, DC 20015, USA, ssheppard@carnegiescience.edu*

[2]*Northern Arizona University, Flagstaff, AZ 86011, USA*

[3]*Institute for Astronomy, University of Hawai'i, Honolulu, HI 96822, USA*

[4]*HL Dodge Department of Physics and Astronomy, University of Oklahoma, Norman, OK 73019, USA*

ABSTRACT

Inner Oort Cloud objects have perihelia beyond the Kuiper Belt with semi-major axes less than a few thousand au. They are beyond the strong gravitational influences of the known planets yet are tightly bound to the Sun such that outside forces minimally affect them. Here we report the discovery of the third known Inner Oort Cloud object after Sedna and 2012 VP113, called 2015 TG387. 2015 TG387 has a perihelion of 65 ± 1 au with a semi-major axis of 1190 ± 70 au. The longitude of perihelion angle for 2015 TG387 is between that of Sedna and 2012 VP113, and thus similar to the main group of clustered extreme trans-Neptunian objects (ETNOs), which may be shepherded into similar orbital angles by an unknown massive distant planet, called Planet X or Planet 9. 2015 TG387's orbit is stable over the age of the solar system from the known planets and Galactic tide. When including simulated stellar encounters to our Sun over 4 Gyrs, 2015 TG387's orbit is still mostly stable, but its dynamical evolution depends on the stellar encounter scenarios used. Surprisingly, when including a massive Planet X beyond a few hundred au on an eccentric orbit that is anti-aligned in longitude of perihelion with most of the known ETNOs, we find 2015 TG387 is typically stable for Planet X orbits that render the other ETNOs stable as well. In fact, 2015 TG387's longitude of perihelion librates about 180 degrees from Planet X's longitude of perihelion in most stable simulations, keeping 2015 TG387 anti-aligned with Planet X over the age of the solar system. We find a power law slope near 3 for the semi-major axis distribution of Inner Oort Cloud objects (IOCs), meaning there are many more high than low semi-major axis IOCs. There are about 2 million IOCs larger than 40 km, giving a mass of 10^{22} kg. The IOCs inclination distribution is similar to the scattered disk, with an average inclination of 19 degs.

Keywords: Kuiper belt: general – Oort Cloud – comets: general – minor planets, asteroids: general – planets and satellites: individual (Sedna, 2012 VP113, 2015 TG387)

1. INTRODUCTION

Extreme Trans-Neptunian objects (ETNOs) have perihelia well beyond Neptune and large semi-major axes ($a > 150 - 250$ au). The ETNOs have only minimal interactions with the known giant

planets and thus are strongly sensitive to gravitational forces hundreds to thousands of au from the Sun. Thus, the ETNOs can be used to probe the solar system beyond the Kuiper Belt (Trujillo and Sheppard 2014).

The ETNOs can be separated into three sub-classes (Figure 1). The scattered ETNOs have perihelia below 38-45 au and likely were created from gravitational scattering with Neptune and still have some significant interactions with Neptune (Brasser & Schwamb 2015). The detached ETNOs have perihelia between about 40-45 to 50-60 au and likely have minimal interactions with the giant planets, but are still relatively close to Neptune and thus could still have significant interactions with the known giant planets (Gladman et al. 2002; Bannister et al. 2017). Inner Oort Cloud objects (IOCs) have perihelia greater than 50-60 au and are too far from the giant planets to be strongly influenced by them (Gomes et al. 2008). The origins of the eccentric IOC orbits likely require mechanisms that operated more efficiently in the past such as stronger outside stellar tide forces or uncatalogued forces in the outer solar system (Fernandez 1997; Brown et al. 2004; Kenyon & Bromley 2004; Madigan et al. 2018; Sefilian & Touma 2018). The orbits of the IOCs thus inform us how the distant solar system formed and currently interacts with its surroundings. The detached ETNOs may have evolved in a similar manner as the IOCs or could be more similar to the scattered ETNOs. Any object with an aphelion beyond a few thousand au is considered an outer Oort cloud object as outside forces such as the Galactic tide and passing stars become strongly significant at these distances (Kaib et al. 2009).

Trujillo and Sheppard (2014) noticed the ETNOs appear to have orbital clustering in their argument of perihelia and were possibly asymmetric in longitude and suggested there is a Super-Earth or larger mass planet beyond a few hundred au shepherding these objects into similar types of orbits. Batygin and Brown (2016a) determined a possible orbit a planet could have to cause the ETNOs to be aligned, with the planet orbit needing to be eccentric, inclined and at several hundred au. After the above works, there have been several more in depth analyses of the ETNOs and how they would evolve and interact under such a massive planet in the outer solar system (Batygin & Morbidelli 2017; Shankman et al. 2017a; Nesvorny et al. 2017; Khain et al. 2018; Hadden et al. 2018; Li et al. 2018). High inclination trans-Neptuninan objects could be created by the planet (Batygin & Brown 2016b). The planet should also cause resonant behavior in the ETNOs (Malhotra et al. 2016; Millholland & Laughlin 2017; Bailey, Brown & Batygin 2018), though the ETNOs may jump between various orbital resonances and configurations (Becker et al. 2017). One of the most interesting behaviors of the ETNOs is the libration of the longitude of perihelion with that of the unknown planet, which was seen in numerical simulations of the ETNO 2013 FT28 by Sheppard and Trujillo (2016). 2013 FT28 was announced after the possible planet orbital parameters were reported by Batygin and Brown (2016a), so 2013 FT28 makes the case stronger that the massive unknown planet beyond a few hundred au exists.

Here we detail the discovery of only the third object with a known perihelion beyond 50 au, 2015 TG387, and how its orbit compares to the other known IOCs and ETNOs. We then discuss the stability of 2015 TG387 through numerical simulations we performed involving the known major planets, Galactic tide, stellar passages and a possible massive Planet X beyond a few hundred au.

2. BASIC SURVEY AND OBSERVATION DETAILS

2015 TG387 was discovered in our ongoing survey for objects beyond the Kuiper Belt edge. This survey is discussed in detail in Trujillo and Sheppard (2014) and Sheppard and Trujillo (2016), where several extreme trans-Neptunian objects were discovered including 2012 VP113, 2014 SR349

and 2013 FT28. Here we report additional fields from the survey (Table 1) and discuss the discovery and implications of 2015 TG387 within these fields, a more detailed paper on the full survey and the discoveries made will follow later.

For discovery, our survey mainly uses the 8.2 meter Subaru telescope (atop Mauna Kea, Hawaii) in the Northern hemisphere with the 1.5 square degree HuperSuprime Camera (HSC) and the 4 meter Blanco telescope (at Cerro Tololo Interamerican Observatory) in the Southern hemisphere with the 2.7 square degree Dark Energy Camera (DECam) (Flaugher et al. 2015). Any objects found beyond about 50 au are recovered months and years later with the 6.5 meter Magellan and 4 meter Discovery Channel Telescope (DCT) to obtain the orbits of the objects. The r-band Subaru HSC images generally have exposure times of about 300 seconds, but exposure times are increased or decreased in order to reach about 25.5 magnitudes in the r-band, depending on the observing conditions for each night. The DECam images use a very wide broad band VR filter and are generally 420 seconds with exposure times varied depending on the observing conditions to reach near 25th magnitude in the r-band. The field depths, time-base and coordinates of the fields are shown in Table 1. Figure 2 shows the field locations on the sky. Table 1 has about 1050 square degrees of new fields, giving the total surveyed area to date about 2130 square degrees when including the fields from Sheppard and Trujillo (2016).

3. DISCOVERY AND ORBIT OF 2015 TG387

2015 TG387 was found near 80 au at Subaru on UT October 13, 2015 with a magnitude of 24.0 in the r-band. Surprisingly, like 2012 VP113, 2015 TG387 is relatively bright compared to the limiting magnitude of most of the survey fields. The Subaru observations generally go deeper than 25.5 mags, making 2015 TG387 about 1.5 mags brighter than the limiting magnitude of the disocovery survey fields it was found in. At 80 au, the expected diameter of 2015 TG387 would be about 300 km assuming a moderate albedo of 15 percent.

2015 TG387 was recovered in December 2015; September, October, November and December 2016; September and December 2017; and May 2018. It thus has multiple observations during 4 separate oppositions. The barycentric orbital elements and their current uncertainties are shown in Table 2. 2015 TG387 has a moderately reliable orbit. Because the semi-major axis has been found to be one of the largest known for a trans-Neptunian object that always stays beyond Neptune, second only to 2014 FE72 (Sheppard and Trujillo 2016), the uncertainties in the orbit of 2015 TG387 are still modest even with the multiple oppositions of observations. We find a semi-major axis of $a = 1190 \pm 70$ au, eccentricity of $e = 0.945 \pm 0.003$, inclination of $i = 11.669 \pm 0.001$ deg, longitude of the ascending node of $\Omega = 300.97 \pm 0.01$ deg, and argument of perihelion of $\omega = 118.2 \pm 0.1$ deg at an epoch of 2457308.8. This makes the argument of perihelion closer to 180 degrees than 0 degrees, which is unlike Sedna, 2012 VP113 and most of the other ETNOs as discussed in Trujillo and Sheppard (2014). In fact, 2015 TG387 is the first detached ETNO or inner Oort cloud object to have an argument of perihelion closer to 180 as opposed to 0 degrees (Figure 3).

3.1. *Longitude of Perihelion of 2015 TG387*

2015 TG387's Longitude of Perihelion is $\bar{\omega} = \omega + \Omega = 59.2 \pm 0.2$ degrees. Trujillo and Sheppard (2014) suggested the inner Oort cloud objects might be asymmetric in longitude, but believed any longitude asymmetries would require further unbiased extreme object discoveries. Batygin and Brown (2016a), using the biased observational results of ETNOs, suggested the longitude of perihelia of

many of the ETNOs are clustered between about 0 and 120 degrees. Sheppard and Trujillo (2016) further examined the longitude of perihelion similarities after discovering more ETNOs in a low biased longitudinal survey. Sheppard and Trujillo (2016) concluded the asymmetry in longitude for the ETNOs is likely real, but still marginal at about the 3 sigma level with the additional discoveries reported in the 2016 paper and assuming all known ETNOs have observational biases similar to their own survey. Additional analysis by Brown (2017) using all the ETNOs with their observational biases further finds the clustering likely real. Shankman et al. (2017b) do not find an obvious longitude of perihelion clustering for ETNOs, though their analysis used a limited set of surveyed longitudes and a liberal definition of what is an ETNO. The Shankman et al. (2017b) results are hindered by a lack of uniform sky coverage and low number statistics, making their results hard to interpret. This is the reason we are performing a very uniform and extensive survey.

Our survey has now covered even more sky since Sheppard and Trujillo (2016) and our longitude biases are now even smaller. 2015 TG387 was found about 45 degrees away in right ascension (RA) on the sky from Sedna and 2012 VP113 and in addition, unlike Sedna and 2012 VP113, was not found within a few au of perihelion but about 15 au away from perihelion at around 80 au. 2015 TG387 is brighter than 25.5 magnitude over an RA range of 22.9 to 9.0 hours, which corresponds to heliocentric distances less than about 100 au, after which 2015 TG387 would be too faint for us to efficiently discover. This means 2015 TG387 could easily have been discovered and/or had a longitude of perihelion well away from the other two known inner Oort cloud objects, but the longitude of perihelion is between Sedna and 2012 VP113. Thus 2015 TG387 continues the longitude clustering trend seen for the inner Oort cloud objects and ETNOs, which might be caused by a massive planet shepherding these objects (Figure 4).

3.2. *Inner Oort Cloud Observational Simulation: Longitude of Perihelion*

Sedna, 2013 VP113 and 2015 TG387 all have similar longitudes of perihelion (96°, 25°, and 59°, respectively). These are the only objects known with perihelion greater than 50 au, where Neptune gravitational effects are mostly insignificant (Gomes et al. 2008, Brasser & Schwamb 2015). Both 2013 VP113 and 2015 TG387 were discovered in our survey, which attempts to have low biases in longitude discovery by observing at all times of the year. We can simulate their detection statistics and biases using methods similar to Sheppard and Trujillo (2016). Sedna is bright enough that almost the whole sky has been searched for such bright objects and thus Sedna can be considered to have no discovery bias in longitude (Brown 2008, Sheppard et al. 2011, Rabinowitz et al. 2012). The observed longitude of perihelion distribution given Sedna, 2015 TG387 and 2013 VP113 is $\bar{\omega} = 60° \pm 35°$ which is a fairly narrow standard deviation.

Assessing whether this observation is consistent with a uniform distribution is not straightforward given the small number of detections and the fact that $\bar{\omega}$ is a continuous angle across the sky. Kuiper's one-sided variation of the Kolmogorov-Smirnov statistic might normally be used, but its statistics are not well defined for number of detections less than 4 (Press et al. 1992), nor is it particularly sensitive with such a low number of detections.

To determine if the longitude of perihelion trend is statistically significant, we first examine a simplistic case where we consider Sedna's longitude of perihelion as an a priori value, then draw two objects (2015 TG387 and 2013 VP113) from a uniform distribution in $\bar{\omega}$ ignoring observational biases. If both objects were within 35°of Sedna's $\bar{\omega}$ then the standard deviation of all three objects would be less than 35°. Assuming binomial statistics this would happen with a probability of $P' =$

$\left(\frac{2\times35^\circ}{360^\circ}\right)^2 = 0.038$, or the equivalent of a 2.1σ assuming Gaussian statistics. This method uses only the 3 known IOCs and does not take observational biases into account.

To simulate observational biases more thoroughly we assume that 2015 TG387 and 2013 VP113 are drawn from the same population of extremely distant objects. We use the distribution detailed in Table 3 as the underlying distribution assuming that the objects have a uniform longitude of perihelion and argument of perihelion. We then tally the number of objects in our observational simulation that would be detected given our combination of survey field sky locations and depths. The resulting survey longitude of perihelion bias is shown in Figure 5. We then assess whether the distribution of $\bar{\omega}$ for the simulated detections is consistent with the actual observed distribution of $\bar{\omega} = 60^\circ \pm 35^\circ$. For this we require that a randomly selected group of two simulated detected objects together with Sedna have a standard deviation of less than 35° and that the mean also differ from 60° by less than 35°. We constructed a simple Monte-Carlo simulation and found that these criteria are satisfied about 5% of the time by a uniform distribution, or about a 2σ significance that the IOCs are not drawn from a uniformly distributed population in longitude of perihelion. As seen in Figure 5 and the results above, our survey has fairly uniform longitude of perihelion discovery statistics as including our observational biases only slightly changes the probability, making an asymmetric population of IOCs a little less significant.

The results in the previous paragraph are for a $q' = 4$ power-law size distribution. We also simulated a $q' = 5$ exponential size distribution and found similar results. We conclude that although the longitude of perihelion clustering continues to appear intriguing, with only 3 known IOCs, several more need to be discovered in low-bias longitude surveys for this effect to be statistically significant at the 3σ level for IOCs.

3.3. *Extreme Trans-Neptunian Object Observational Simulation: Longitude of Perihelion*

We now include the discovery statistics of the detached Extreme Trans-Neptunian Objects (ETNOs) along with the IOCs from our survey. The detached ETNOs can be observationally differentiated from the IOCs because of their more moderate perihelia ($40-45$ au $< q < 50-60$ au) compared to the IOCs' extremely high perihelia of $q > 50 - 60$ au. The detached ETNOs may have similar formation and evolutionary histories as the IOCs, but they are significantly closer to the giant planets, and thus could have obtained their orbits through different processes (Brasser & Schwamb 2015, Bannister et al. 2017). Assuming a $q > 40 - 45$ au and $a > 150 - 250$ au definition for the detached ETNOs, the detached ETNOs found in our survey are safely 2014 SR349 and if less conservative also 2013 FT28 (Table 2). We also found several ETNOs that have lower perihelia than 40 au and thus are not detached but scattered ETNOs with more interactions with Neptune: 2014 FE72, 2013 UH15, 2013 FS28, and 2014 SS349. These scattered ETNOs were detailed in Sheppard and Trujillo (2016) and here we only consider the detached ETNOs 2014 SR349 and 2013 FT28, and in the most conservative case we only consider 2014 SR349, with its perihelion above 45 au and semi-major axis above 250 au.

The statistics for the longitude of perihelion clustering improve by including 2014 SR349 with the discovery statistics computed above for IOCs Sedna, 2015 TG387 and 2012 VP113. For this group of objects, the mean $\bar{\omega} = 49^\circ \pm 36^\circ$. We computed the significance of this in the simple case by running a Monte Carlo simulation with our three detections and Sedna drawn from a uniform distribution in $\bar{\omega}$ and ignoring observational bias. Only 1.5% of the time do these three objects have $\bar{\omega}$ close enough to Sedna for the mean of all objects to be within $49^\circ \pm 36^\circ$ and the standard deviation to be

$< 36°$, the equivalent of a 2.4σ event in Gaussian statistics. Using our observational bias simulator and the method in Section 3.2, we find that these criteria are met only $P = 2.8\%$ of the time when the ETNOs and IOCs are drawn from a uniform $\bar{\omega}$ distribution. This is the equivalent of 2.2σ in the Gaussian case, which again is interesting but not statistically significant at the 3σ level since only four objects are used in the analysis.

Using the more liberal definition in perihelion of a detached ETNO of $q > 40$ au and $a > 250$ au would cause 2013 FT28 to be included in the detached ETNO group as well. The orbit of 2013 FT28 has $\bar{\omega} = -101.860°$, which departs from the mean of the other IOCs and ETNOs by about 180 degrees. Sheppard and Trujillo (2016) proposed 2013 FT28 is the first known ETNO aligned with Planet X in longitude of perihelion. A distant massive planet on an elongated orbit would likely create both an anti-aligned and aligned longitude of perihelion population of ETNOs with respect to the Planet's longitude of perihelion (Brown and Batygin 2016a). That is, the aligned population has a longitude of perihelion similar to that of the hypothesized planet on an elongated orbit while an anti-aligned population would differ by about 180°.

If we make the assumption that 2013 FT28 is a member of the opposite ETNO population than Sedna, 2012 VP112, 2015 TG387 and 2014 SR349, its longitude of perihelion does indeed fit the $\bar{\omega}$ pattern already discussed as $180° - 101.86° = 78.14°$, which is well within the mean $\bar{\omega}$ for the other ETNOs and IOCs ($49° \pm 36°$). If this were the case, this would decrease the probability that $\bar{\omega}$ for the ETNO and IOCs were drawn from a random uniform distribution. From our observational bias simulation, this would suggest $P = 0.013$ or 2.5σ in Gaussian statistics. Again, not yet statistically significant as there are only a few objects used, but cause for interest.

Above we are trying to use only objects found in low longitude bias surveys, but very few objects have been found like this and is the main reason we are continuing our survey. Taking all known conservatively defined detached ETNOs and IOCs ($q > 45$ au and $a > 250$ au) into account finds 8 objects (Sedna, 2012 VP113, 2015 TG387, 2004 VN112, 2010 GB174, 2013 SY99, 2014 SR349 and 2015 RX245), all with longitude of perihelion between 15 and 120 degrees. This has a 0.005% chance of happening and is about a 4σ event, if ignoring possible observational biases. So again, the longitude of perihelion clustering is interesting, but further low biased discoveries are needed.

3.4. *The Inner Oort Cloud Semi-Major Axis Distribution*

We have detected two IOCs in our survey with very different semi-major axes, 2015 TG387 with $a = 1190$ au and 2012 VP113 with $a = 270$ au. This suggests a semi-major axis distribution that has more distant objects than the a^1 assumed by Sheppard and Trujillo (2016), a value that was largely assumed due to limited discovery statistics. Since solar system volume increases with heliocentric distance as R^3, although a a^1 semi-major axis distribution has more objects with large semi-major axis than small, the real underlying space density of objects for a a^1 distribution would fall as R^{-2}. According to our observational bias simulations, assuming a^1 one would expect to find about 23 objects within 10 au of 2012 VP113's low semi-major axis for every object within 10 au of 2015 TG387's high semi-major axis. Since the number of true detections is only 2, we cannot statistically rule out the possibility of a a^1 semi-major axis distribution. However, we find that to observe equal numbers of $a = 270$ au and $a = 1190$ au objects we would have to draw them from an $\sim a^{2.7}$ semi-major axis distribution. Such a semi-major axis distribution would imply a much larger number of IOCs and a population that is highly dependent on the number of very distant objects, which are the most difficult to observe. All other parameters remaining the same, this $a^{2.7}$ population would

have to be a factor ~ 2 larger than an a^1 population. We use this $a^{2.7}$ semi-major axis distribution as our favored semi-major axis distribution for the remainder of this work. Interestingly, if the true semi-major axis distribution is close to power law of exponent 3, as these simulations suggest, this implies a fairly constant space density of objects moving outward with distance.

3.5. *Population Number and Mass of IOCs*

From the observational simulations we find that the total number of IOC objects is quite large, mainly because IOCs can only be detected for a small fraction of their orbits. For 2015 TG387, assuming a semi-major axis of 1190 au and a perihelion of 65 au, 2015 TG387 will be fainter than our faintest HSC survey field depths, $r \sim 25.5$ mags, for 99.5% of its orbital period. Using our observational bias simulation with a variety of parameters (combinations of $q = 4, 5$ and $a = 2.7$), the total number of objects larger than radius 20 km based on our 2 detections (2015 TG387 and 2012 VP113) is roughly 2×10^6 with total mass of about 10^{22} kg. This total mass likely exceeds that of Classical dynamically "cold" TNOs and is similar to the dynamically "hot" TNOs which have mass of about $M = 1.8 \times 10^{21}$ kg and 6.0×10^{22} kg, respectively (Fraser et al. 2014). This is a lower limit on the IOC mass given that we have almost no constraints on distant, low eccentricity objects which are unobservable given current technology. Sheppard and Trujillo (2016) showed the Cumulative Luminosity Function and size distribution of the ETNOs and IOCs are likely similar to the Kuiper Belt as well.

3.6. *Observational Bias Simulation: Inclination Distribution*

The inclinations of our IOCs and detached ETNOs are moderate, between $11.7^\circ < i < 24.0^\circ$. Our survey observed mostly between 5 and 25 degrees from the ecliptic, though we did approach the ecliptic and thus were sensitive to objects with inclinations significantly lower than that detected. We can say that the inclination distribution of the IOCs and detached ETNOs is quite thick, and in fact in our survey simulation we use the inclination distribution for the scattered disk objects as found by Gulbis et al. 2010 ($\mu_1 = 19.1^\circ$ and $\sigma_1 = 6.9^\circ$) as this is similar to the average ETNO inclination found by Sheppard and Trujillo (2016). Our observational bias simulator suggests that the observed ETNO/IOC inclination distribution is consistent with the inclination distribution of the scattered disk objects.

We can rule out narrow distributions for the ETNOs/IOCs. For instance, our observations are not consistent with the more inclined component of the Classical KBOs ($\sigma_3 = 8.1^\circ$, Gulbis et al. 2012). The simulated detected distribution in this case has a mean inclination of $i = 10.5^\circ \pm 4.8^\circ$. This is inconsistent with the detection of 2012 VP113 with an inclination of $i \sim 24^\circ$. From our observational bias simulation, the probability of us discovering an object with $i > 24^\circ$ is 0.0032, which is ruled out at the 3σ level assuming Gaussian statistics. Given this and the fact that 2013 FT28 and 2014 SR349 have inclinations $i > 17$ which each have a probability of discovery of only 0.22, we can reject the hypothesis that the ETNOs/IOCs follow the inclination distribution of the Classical TNO populations at the $> 3\sigma$ level.

We can also say that the IOCs and detached ETNOs likely do not have a high inclination distribution like that found for TNOs with perihelia above 40 au and experiencing both Neptune Mean Motion Resonance (MMR) and Kozai Resonance (KR) behavior. These MMR-KR objects have an average $i \sim 28^\circ$ (Sheppard et al. 2016) and we have found no detached ETNOs or IOCs with inclinations this high while finding several even more inclined MMR-KR objects in the same survey. One

very high inclination scattered ETNO has been found, 2015 BP519 with an inclination of 54 deg, but this object has a fairly low perihelion near Neptune and thus may not be related to the IOCs and detached ETNOs with much higher perihelia (Becker et al. 2018).

4. SIMULATIONS OF 2015 TG387'S ORBIT STABILITY

We ran several numerical simulations to determine the orbit stability of 2015 TG387 over the age of the solar system under differing conditions. In all simulations, we used the nominal orbit of 2015 TG387 and clones within 3 sigma of the nominal orbit when including the orbital uncertainties.

4.1. *2015 TG387's Stability With Known Major Planets*

We found the orbit of 2015 TG387 is very stable when including only the 4 giant planets and the Sun in our numerical simulations using the Mercury program (Chambers 1999). 2015 TG387's semi-major axis, eccentricity and inclination change little over the age of the solar system (Figure 6). 2015 TG387's longitude of perihelion, argument of perihelion and longitude of the ascending node cycle or precess through 360 degrees from the minor interactions with the quadrupole of the solar system's potential. For 2015 TG387, the time-scale for the argument of perihelion and longitude of perihelion cycle is about 4 and 6.5 Gyr, respectively, when just including the 4 giant planets. This precession is true for all ETNOs that remain beyond Neptune for their entire orbit, though the cycle time-scales differ depending on the object semi-major axis and perihelion distance as an object with higher semi-major axis and/or higher perihelion will have less interactions with the known giant planets and thus take longer to precess (Trujillo and Sheppard 2014). See below for a further discussion of the longitude of perihelion and the ETNOs' precession about these angles for various different simulations.

4.2. *2015 TG387's Orbit with Galactic Tide*

To better understand the long-term dynamical behavior of 2015 TG387 to forces outside of the Solar System, we integrated 100 clones of 2015 TG387 in the presence of the known giant planets and Galactic tide for 4 Gyrs. An example of the evolution of one of these clones is shown in Figure 7. We also compare it with the evolution of Sedna, 2012 VP113, and 2014 FE72. As can be seen in the figure, the perihelion of 2015 TG387 can fluctuate by $\sim \pm 10$ au over the course of 4 Gyrs due to influence from the Galactic tide. When the 2015 TG387 clone is driven down to a perihelion of $\sim$60 AU, the object begins receiving small energy kicks from the giant planets, driving a minor diffusion in its semi-major axis, which then restabilizes when the perihelion rises above $\sim$60 AU again. In contrast, Sedna has very small changes in perihelion as its aphelion is only about 1000 au while 2012 VP113 undergos almost no changes in perihelion due to its much smaller semi-major axes, which limits the effects of the Galactic tide. Their non-evolving, larger perihelia result in semi-major axes that are virtually fixed with time. On the other hand, 2014 FE72 has a much smaller perihelion and a larger semi-major axis than 2015 TG387. Within a couple hundred Myrs, its perihelion has moved even closer to the planets leading to its ejection from the solar system.

The behavior of 2014 FE72 demonstrates that if 2015 TG387 evolves too much in perihelion its semi-major axis can be inflated via planetary perturbations to the point where it becomes unstable due to wild swings in pericenter driven by the Galactic tide when the semi-major axis is large. However, our integrations of clones demonstrate that such behavior is unlikely for 2015 TG387 as it has a significantly high perihelion and low semi-major axis to prevent major changes to its orbit from

both inside and outside forces. Out of our 100 clones, only one was ejected from the solar system over 4 Gyrs of evolution (a clone near the 3σ uncertainty limit), and during the last Gyr of integration any given clone only had a 0.8% chance of having $q < 55$ AU.

When including the outside forces from the Galactic tide with the known major planets in our simulations, 2015 TG387's orbit is mostly stable, though there is a little more movement in its semi-major axis, eccentricity and inclination from some minor interactions with the Galactic tide than without the Galactic tide simulations. Only a few percent of the clones have significant movement of some 10 au in perihelion and 100 au in semi-major axis over 4 Gyrs, but all but one have their perihelia still above 55 au. We consider 2015 TG387 to be stable to the Galactic tide.

4.2.1. *The Combination of the Galactic Tide and Solar System's Quadrupole Moment on Orbit Stability of ETNOs*

Our above results show that outside forces work in tandem with inside forces when an object has a perihelion less than 60 au and a semi-major axis above 1000 au. The amount the Galactic tide affects an ETNOs orbit is a complicated function of the semi-major axis, inclination and perihelion distance of the object. The higher the semi-major axis the more the Galactic tide becomes important, with objects beyond 1000 au starting to have significant interactions with the Galactic tide as shown by Sedna in Figure 7 (see also Duncan et al. 2008; Kaib & Quinn 2009; Soares & Gomes 2013). If just the Galactic tide was important, one could calculate an object's perihelion change over time based on the object's semi-major axis and inclination (see Heisler & Tremaine 1986). But the perihelion distance is also very important for the stability of an object as once it drops below about 60 AU, interactions with the known giant planets become important as shown by the simulations of 2015 TG387's orbit (Figure 7). These interactions deliver weak energy kicks driving a diffusion in semimajor axis. If the semimajor axis increases, then the Galactic tide can drive the perihelion even closer to the planets, generating stronger energy kicks. If the perihelion drops near or below 30-35 au, the object will likely become unstable from strong gravitational interactions with the giant planets, like found for 2014 FE72.

Thus an object with a higher perihelion but similar distant semi-major axis is more stable since the object would have similar Galactic tide interactions from outside forces but less interactions with the known giant planets. But there is also the precession effect from the quadrupole moment of the giant planets interaction to consider. An object with faster solar system precession of its orbital angles, most importantly its argument of perihelion as this angle determines the sign of the Galactic tide perturbation, makes the Galactic tide perihelion perturbation shift from positive to negative and back over time, having a canceling effect on the Galactic tide. The cycling of the argument of perihelion from just the giant planets can be seen in Figure 6, while the fluctuation of the perihelion from the Galactic tide going positive to negative can be seen in Figure 7.

A slow precession of the argument of perihelion, with the critical period being longer than the age of the solar system, will not allow the precessing to suppress net Galactic tide perturbations and thus the Galactic tide perturbations just become larger over time, so tidal shifts get larger causing the perihelion to have larger movement. An object will have slower precession with a higher perihelion or higher semi-major axis since it will interact less with the known inner giant planets.

2015 TG387 is near the limits of stability, but appears to be a mostly stable object. Its semi-major axis and aphelion distance are large enough to cause significant interactions with outside forces, but its perihelion is just high enough that the fluctuations of its perihelion keep it from strongly

interacting with the giant planets. If 2015 TG387 had a little lower perihelion distance or little higher semi-major axis, it would be a much more unstable orbit from the combination of outside and inside forces.

4.3. *2015 TG387's Orbit with Galactic Tide and Passing Stars*

We further ran several simulations that included nearby passing stars as well as the galactic tide and 4 known giant planets for 4 Gyrs. The passing star parameters were chosen to be similar as that found in Rickman et al. (2008) and were meant to mimic the conditions of the solar neighborhood. Because the process of generating random field stars has an inherent element of stochasticity, we generated four different sets of field star encounters and integrated our 2015 TG387 clones under each set separately.

Unlike in the simulations with only the giant planets and the Galactic tide, here we see some of the clones have more significant evolution. The four different simulations gave somewhat different results as our clone survival rates after 4 Gyrs of integration for each stellar passage simulation were 99%, 95%, 94% and 35%. Thus we do find there is additional pericenter evolution from passing stars that drives more of our clones into interacting with the giant planets, but the median case still has the vast majority of clones surviving. If we select the 95% survival simulation as our fiducial case, at any given point in the last Gyr of integration a clone has a ∼16% chance of having $q < 50$ AU. However, the majority (63%) of our clones maintained a perihelion larger than 50 AU for the entire last Gyr of the integration, indicating that under many stellar passage scenarios, the orbit of 2015 TG387 can remain stable for the age of the solar system. 2015 TG387 Clone 1 in Figure 8 displays the evolution with the moderate stellar encounter scenario where 95% of the 2015 TG387 clones survived, showing minimal changes in the orbit of 2015 TG387 Clone 1 over the age of the solar system.

The other object's evolution shown in Figure 8 come from the simulation with the most powerful set of stellar encounters (35% of 2015 TG387 clones survived). For 2015 TG387 Clone 2, powerful stellar encounters alter the orbit around ∼100 Myrs and ∼900 Myrs (Figure 8). After this, a combination of perturbations from additional stellar passages and the Galactic tide drive Clone 2's perihelion into the planetary region where it begins receiving strong energy kicks from the giant planets. This ultimately leads to its ejection after ∼3 Gyrs. In this particular simulation, such behavior like Clone 2's is not rare, as only 35% of our clones survive the simulation. However, as previously noted, each set of stellar encounters is unique and their overall cumulative effect is strongly dependent on the few most powerful stellar passages. One can see this when we study the evolution of Sedna and 2012 VP113 in the same simulation (Figure 8). Although Sedna and 2012 VP113 have more strongly bound orbits to the Sun and are generally assumed to be very stable, a particularly powerful set of encounters can elicit some evolution (of order ∼5 AU) in their perihelia, as was found in Kaib et al. (2011).

4.4. *2015 TG387's Orbit with a distant Planet X*

Next we ran simulations to determine if 2015 TG387 could be stable to the possible distant unknown massive planet beyond a few hundred au that may be shepherding the ETNOs into similar types of orbits (Trujillo and Sheppard 2014, Batygin and Brown 2016a). In order to identify where the planet might be in the sky, Trujillo (2018) ran thousands of simulations of a possible distant planet using the orbital constraints put on this planet by Batygin and Brown (2016a). The simulations varied the orbital parameters of the planet to identify orbits where known ETNOs were most stable. Trujillo

(2018) found several planet orbits that would keep most of the ETNOs stable for the age of the solar system.

To see if 2015 TG387 would also be stable to a distant planet when the other ETNOs are stable, we used several of the best planet parameters found by Trujillo (2018). In most simulations involving a distant planet, we found 2015 TG387 is stable for the age of the solar system when the other ETNOs are stable. This is further evidence the planet exists, as 2015 TG387 was not used in the original Trujillo (2018) analysis, but appears to behave similarly as the other ETNOs to a possible very distant massive planet on an eccentric orbit. We depict the evolution of 2015 TG387's orbit with the most favorable distant giant planet orbit from Trujillo (2018) in Figure 9.

4.4.1. *Longitude of Perihelion Coupled to Planet X*

The longitude of perihelion angle for a distant object beyond Neptune will generally precess from the minor gravitational interaction of the object with the quadrupoles of the known major planets. The time to make one complete revolution through the longitude of perihelion angles depends on the object perihelion distance and semi-major axis. The more distant an object's perihelion and/or semi-major axis the slower the object will precess in longitude of perihelion. It takes about 1.3 Gyr for 2012 VP113's longitude of perihelion to precess 360 degrees, while it takes 3.0 Gyr for Sedna. We find 2015 TG387 takes about 6 billion years to precess 360 degrees in longitude of perihelion when taking just the known major planets into account. The hypothetical distant massive planet with a perihelion of $\sim$ 200 au and semi-major axis of $\sim$ 700 au precesses very slowly in longitude of perihelion because of its distant perihelion and semi-major axis, moving only about 15 degrees over the age of the solar system in longitude of perihelion.

In our simulations where 2015 TG387 was stable with the additional massive distant unknown planet, we found that 2015 TG387 frequently does not precess on a 6 billion year time-scale in longitude of perihelion but librates near its current longitude of perihelion, keeping it mostly anti-aligned with the hypothetical planet for the age of the solar system. This keeps the object away from crossing the planet's orbit and thus stable. Amazingly, these distant planet orbits were not chosen to make 2015 TG387 stable, but were simply the planet orbits found in Trujillo (2018) that kept the other ETNOs mostly stable over the age of the solar system. 2015 TG387 was only added in the simulations after its orbit was well determined, which was after the Trujillo (2018) simulation results were determined.

This is surprising to find that the third known inner Oort cloud object is stable with the distant massive planet orbits found for the other inner Oort cloud objects and ETNOs, and not only is 2015 TG387 stable, but it has resonance behavior with its longitude of perihelion, librating 180 degrees from the planet's. Though this does not prove the hypothetical distant planet first realized by Trujillo and Sheppard (2014) and further revealed by Batygin and Brown (2016a) is real, it is strongly suggestive.

We also found that in most of the dynamical simulations with planet X, some 2015 TG387 clones became retrograde while still being in a stable orbit in resonance with the hypothesized planet with the longitude of perihelion still constrained to be anti-aligned with the planet (Figure 10). Thus finding retrograde ETNOs could be a further signature of planet X if they too are clustered into certain orbital configurations. This also suggests the distant planet itself could be on a retrograde orbit. To test this theory, we reran all of our simulations that involved Planet X, but this time put the distant planet on a retrograde orbit, with all other variables being the same. This involved changing

the Planet X orbital elements inclination to $i_{retrograde} = 180° - i_{prograde}$, longitude of the ascending Node to $\Omega_{retrograde} = 180° - \Omega_{prograde}$, argument of perihelion to $\omega_{retrograde} = 180° - \omega_{prograde}$, and mean anomaly to $M_{retrograde} = -M_{prograde}$. We found that 2015 TG387 behaves very similar to a retrograde Planet X as it does to a prograde Planet X (Figure 11). 2015 TG387 continues to be stable and confined in longitude of perihelion and argument of perihelion angles even with a retrograde Planet X. We found this true for all the ETNOs.

4.5. *Stability of 2015 TG387 with Planet X, Galactic Tides and Passing Stars*

When adding in Galactic tides with the simulations involving 2015 TG387 and a distant planet, we find most clones of 2015 TG387 continue to librate in longitude of perihelion. Thus Galactic tides are not a destabilizing force to 2015 TG387's libration in longitude of perihelion with the planet.

In the passing stars case, where outside perturbations can be much stronger and stochastic, we also found a large percentage of 2015 TG387 clones librating in longitude of perihelion with the planet for the age of the solar system. In a 4-Gyr simulation using our fiducial 95% 2015 TG387 clone survival stellar encounter set with the Galactic tide and a distant planet, we find that the survival fraction of 2015 TG387 clones drops to 72%. However, of those surviving clones, 68% have a longitude of perihelion that is $\pm 45°$ of being exactly anti-aligned with the planet's longitude of perihelion $\sim 180°$ away, showing the surviving 2015 TG387 clones are the ones that have longitude of perihelion resonance with the planet as found in the previous Planet X simulations.

5. SUMMARY

We discovered a new Inner Oort Cloud object (IOC), 2015 TG387, that has the third highest perihelion of any known object to date at 65 ± 1 au. 2015 TG387 was discovered in our ongoing survey for objects beyond 50 au, which has now covered 2130 square degrees of sky mostly using the Subaru 8m and Blanco 4m telescopes. Assuming a moderate albedo, the diameter of 2015 TG387 is about 300 km. The details on this new discovery are:

1) 2015 TG387's longitude of perihelion of 59 degrees is similar to Sedna, 2012 VP113 and the other ETNOs. Using only the low observationally biased discovered IOCs and detached ETNOs from our survey as well as Sedna finds the longitude of perihelion clustering only about a 2 to 2.5 σ significance. The significance of the clustering is not at the 3σ level because only four objects are being used that have low observational biases in their longitude discovery (Sedna, 2012 VP113, 2015 TG387 and 2014 SR349). Using all 8 of the known IOCs and detached ETNOs gives a significance of $\sim 4\sigma$ in longitude of perihelion clustering, but this ignores the longitude biases in the discovery of many of these objects. Several more IOC and detached ETNOs need to be discovered in uniform longitude surveys to obtain a good statistical analysis of the population's longitude of perihelion clustering. The longitude of perihelion clustering continues to be an interesting trend to watch.

2) With the discovery of 2015 TG387, we find the semi-major axis distribution of the IOCs is likely an $a^{2.7}$ distribution. That is, there are many more IOCs with high semi-major axes than low semi-major axes. If the power law slope of the semi-major axis distribution is near 3 as we suggest, this implies a fairly constant space density of objects moving outwards with distance since the volume of space goes as the cube of distance.

3) The total number of the IOCs larger than 40 km in diameter is about 2×10^6, giving a total mass of about 10^{22} kg. This makes the IOC population similar in mass to the Kuiper Belt population when using a size distribution as shown in Sheppard and Trujillo (2016).

4) The IOCs and detached ETNOs appear to have an inclination distribution similar to the scattered disk population of TNOs, with an average inclination around 19 degrees. The IOCs do not appear to have a narrow (like the classical KBOs) or very thick (like the MMR-KR TNOs) inclination distribution as most have inclinations between about 10 and 25 degrees inclination.

5) 2015 TG387 has a very stable orbit when just simulating the known planets in our solar system. The orbit is also fairly stable when including the galactic tide. Including passing stars over the age of the solar system finds 2015 TG387 usually stable as well, but it is dependent on the stellar encounter scenario used. In most stellar encounter scenarios, some 95% of 2015 TG387 clones are stable for the age of the solar system. But in the strongest stellar encounter scenario used, some 65% of 2015 TG387 clones are lost over the age of the solar system. Overall, 2015 TG387 appears to be on an orbit that most likely has lasted the age of the solar system near its current orbital parameters.

6) We find the outside force of the Galactic tide and inside force of the quadrupole moment of the solar system work in tandem to effect 2015 TG387's orbit. The Galactic tide becomes important beyond about 1000 au, as seen in Sedna's orbit evolution. The quadrupole moment of the solar system is important when the precession of the angle of argument of perihelion of an object's orbit is slow enough that the Galactic tide perturbations continually increase until an object's perihelion is pushed interior to about 60 au. Once an object has a perihelion interior to $\sim$ 60 au, significant energy kicks from the known giant planets cause an object's semi-major axis to change. This change in semi-major axis can have increased energy kicks from the giant planets that can further lower the perihelion of an object until it starts to more strongly interact with the giant planets. Once the perihelion of an object is around 30-35 au or lower, the object will likely become unstable from gravitational scattering off the giant planets.

2015 TG387 is near the edge of stability because it is near the perturbations from both inside and outside forces. That is, 2015 TG387's perihelion is just high enough that interactions with the giant planets are not significant, though its semi-major axis is just large enough that Galactic tide perturbations can push 2015 TG387's perihelion a little interior to 60 au causing slight semi-major axis variations. But as 2015 TG387's argument of perihelion precesses from interactions with the quadrupole moment of the solar system, the perihelion of 2015 TG387 will rise back above 60 au before any significant changes in its orbit from giant planet energy kicks while it has a perihelion below 60 au. If 2015 TG387 had a little closer perihelion or little larger semi-major axis, it would be more unstable as it would be pushed into interacting more with the giant planets. If an object gets its perihelion pushed down to around 30-35 au or lower, it will become unstable from strong gravitational interactions with the giant planets. Thus objects that have moderate semi-major axes and are generally thought to be stable in the inner Oort cloud (1000 to 2000 au) can still become unstabilized fairly easily if they have perihelia that can be pushed well below about 60 au from a combination of outside and inside forces. The main cause of an ETNO or IOC obtaining an unstable orbit is the strong interactions it can have with the giant planets when its perihelion is eventually pushed to around 30 au or less.

7) When including a massive Planet X at several hundred astronomical units as predicted by Trujillo and Sheppard (2014) with the eccentric and inclined rudimentary orbit proposed for it by Batygin and Brown (2016a) in our simulations, we find 2015 TG387 is usually stable to such a planet when the other IOCs and ETNOs are also stable. Amazingly, in most simulations with a Planet X, we found 2015 TG387 librates in its longitude or perihelion, keeping it anti-aligned and thus stable with

the eccentric Planet X for the age of the solar system. This longitude of perihelion libration is not seen in the the simulations without a Planet X. This supports the theory that a Planet X exists as 2015 TG387's orbit was only determined after the basics of the Planet X orbit was realized, yet 2015 TG387 reacts with the planet very similarly to the other known IOCs and ETNOs. In addition, some 2015 TG387 clones obtain retrograde orbits yet still remain stable and anti-aligned with planet X for the age of the solar system, suggesting retrograde ETNOs should exist in most planet X scenarios. We further found that the planet itself might be on a retrograde orbit as 2015 TG387 and other ETNOs were similarly stable as in the prograde planet case.

ACKNOWLEDGMENTS

Based in part on data collected at Subaru Telescope, which is operated by the National Astronomical Observatory of Japan. Observations were partly obtained at Cerro Tololo Inter-American Observatory, National Optical Astronomy Observatory, which are operated by the Association of Universities for Research in Astronomy, under contract with the National Science Foundation. This project used data obtained with the Dark Energy Camera (DECam), which was constructed by the Dark Energy Survey (DES) collaborating institutions: Argonne National Lab, University of California Santa Cruz, University of Cambridge, Centro de Investigaciones Energeticas, Medioambientales y Tecnologicas-Madrid, University of Chicago, University College London, DES-Brazil consortium, University of Edinburgh, ETH-Zurich, University of Illinois at Urbana-Champaign, Institut de Ciencies de l'Espai, Institut de Fisica d'Altes Energies, Lawrence Berkeley National Lab, Ludwig-Maximilians Universitat, University of Michigan, National Optical Astronomy Observatory, University of Nottingham, Ohio State University, University of Pennsylvania, University of Portsmouth, SLAC National Lab, Stanford University, University of Sussex, and Texas A&M University. Funding for DES, including DECam, has been provided by the U.S. Department of Energy, National Science Foundation, Ministry of Education and Science (Spain), Science and Technology Facilities Council (UK), Higher Education Funding Council (England), National Center for Supercomputing Applications, Kavli Institute for Cosmological Physics, Financiadora de Estudos e Projetos, Fundao Carlos Chagas Filho de Amparo a Pesquisa, Conselho Nacional de Desenvolvimento Cientfico e Tecnolgico and the Ministrio da Cincia e Tecnologia (Brazil), the German Research Foundation-sponsored cluster of excellence "Origin and Structure of the Universe" and the DES collaborating institutions. This paper includes data gathered with the 6.5 meter Magellan Telescopes located at Las Campanas Observatory, Chile. This research was funded by NASA Planetary Astronomy grant NN15AF446.

REFERENCES

Bailey, E., Brown, M., Batygin, C. 2018, AJ, 156, 74-79.
Bannister, M., Shankman, C., Volk, K. et al. 2017, AJ, 153, 262.
Batygin, K. & Brown, M. 2016a, AJ, 151, 22.
Batygin, K. & Brown, M. 2016b, ApJ, 833, 3.
Batygin, K. & Morbidelli, A. 2017, AJ, 154, 229.
Becker, J., Adams, F., Khain, T., Hamilton, S. & Gerdes, D. 2017, AJ, 154, 61.
Becker, J., Khain, T., Hamilton, S. et al. 2018, AJ, 156, 81.
Brasser, R. & Schwamb, M. 2015, MNRAS, 446, 3788.
Brown, M., Trujillo, C. & Rabinowitz, D. 2004, ApJ, 617, 645.
Brown, M. 2008, in The Solar System Beyond Neptune, ed. M. Barucci, H. Boehnhardt, D. Cruikshank and A. Morbidelli (Tucson: Univ of Arizona Press), 335-344.
Brown, M. & Batygin, K. 2016, ApJ, 824, 23.
Brown, M. 2017, AJ, 154, 65.
Chambers, J. 1999, MNRAS, 304, 793.
Duncan, M., Brasser, R., Dones, L., and Levison, H. 2008, in The Solar System Beyond Neptune, eds. M. Barucci, H. Boehnhardt, D. Cruikshank and A. Morbidelli (Tucson: Univ of Arizona Press), 315-331.
Fernandez, J. 1997, Icarus, 129, 106.
Flaugher, B., Diehl, H., Honscheid, K., et al. 2015, AJ, 150, 150.

Gladman, B., Holman, M., Grav, T., Kavelaars, J., Nicholson, P., Aksnes, K. & Petit, J. 2002, Icarus, 157, 269.
Gomes, R., Fernandez, J., Gallardo, T., & Brunini, A. 2008, in The Solar System Beyond Neptune, ed. M. Barucci et al. (Tucson, AZ: Univ. Arizona Press) pp. 259273
Gulbis, A., Elliot, J., Adams, E., Benecchi, S., Buie, M. Trilling, D., and Wasserman, L. 2010, AJ, 140, 350-369.
Hadden, S., Li, G., Payne, M., & Holman, M. 2018, AJ, 155, 249.
Heisler, J. & Tremaine, S. 1986, Icarus, 65, 13.
Holman, M., Payne, M., Fraser, W. et al. 2018, ApJ, 855, L6.
Kaib, N., Becker, A., Jones, L. et al. 2009, ApJ, 695, 268.
Kaib, N. and Quinn, T. 2009, Science, 325, 1234.
Kaib, N., Roskar, R., & Quinn, T. 2011, Icarus, 215, 491.
Kaib, N. & Sheppard, S. 2016, AJ, 152, 133.
Kenyon, S. & Bromley, B. 2004, Nature, 432, 598.
Khain, T., Batygin, K. & Brown, M. 2018, AJ, 155, 250.
Li, G., Hadden, S., Payne, M. & Holman, M. 2018, arXiv:1806.068687.
Madigan, A., Zderic, A., McCourt, M. & Fleisig, J. 2018, arXiv:1805.03651.
Malhotra, R., Volk, K. & Wang, X. 2016, ApJ, 824, L22.
Morbidelli, A. and Levison, H. 2004 ApJ, 128, 2564.
Millholland, S. & Laughlin, G. 2017, AJ, 153, 91.
Nesvorny, D., Vokrouhlicky, D., Dones, L., Levison, H., Kaib, N. & Morbidelli, A. 2017, ApJ, 845, 27.
Press, W., Teukolsky, S., Vetterling, W., Flannery, B. 1992, in Numberical Recipes in C: The Art of Scientific Computing, Second Edition. (Cambride University Press) pp. 623-628.
Rabinowitz, D., Schwamb, M., Hadjiyska, E., and Tourtellotte, S. 2012, AJ, 144, 140.
Rickman, H., Fouchard, M., Froeschle, C., Valsecchi, G. 2008, CeMDA, 102, 111.
Sefilian, A. & Touma, J. 2018, arXiv:1804.06859.
Shankman, C., Kavelaars, J., Lawler, S., Gladman, B. & Bannister, M. 2017a, AJ, 153, 63.
Shankman, C., Kavelars, J., Bannister, M. et al. 2017b, AJ, 154, 50.
Sheppard, S., Udalski, A., Trujillo, C. et al. 2011, AJ, 142, 98.
Sheppard, S., Trujillo, C., & Tholen, D. 2016, ApJ, 825, L13.
Sheppard, S. & Trujillo, C. 2016, AJ, 152, 221.
Soares, J., and Gomes, R. 2013, AA, 553, 110.
Trujillo, C. & Sheppard, S. 2014, Nature, 507, 471.
Trujillo, C. 2018, ApJ, submitted.

Table 1. Further Inner Oort Cloud Survey Observations

UT Date	Telescope	T	θ	Limit	Area
yyyy/mm/dd		(hrs)	(“)	(m_r)	(deg^2)
2015/10/12	Subaru	$3-5$	$0.45-0.7$	25.9	49.5
	hsc216	23:26:44	+11:39:00		
	hsc204	23:30:56	+13:51:00		
	hsc199	23:32:20	+10:39:00		
	hsc292	00:04:56	+09:57:00		
	hsc281	00:01:20	+12:57:00		
	hsc302	00:07:20	+12:03:00		
	hsc336	00:18:20	+12:21:00		
	hsc367	00:26:44	+14:00:00		
	hsc383	00:30:44	+12:36:00		
	hsc410	00:38:32	+14:12:00		
	hsc432	00:43:56	+13:06:00		
	hsc448	00:48:20	+14:27:00		
	hsc475	00:56:20	+14:45:00		
	hsc481	00:58:20	+16:33:00		
	hsc507	01:05:20	+17:03:00		
	hsc527	01:12:20	+17:27:00		
	hsc550	01:18:32	+16:36:00		
	hsc568	01:23:56	+17:48:00		
	hsc585	01:28:44	+16:30:00		
	hsc625	01:39:32	+18:42:00		
	hsc651	01:46:44	+19:03:00		
	hsc689	01:57:32	+19:54:00		
	hsc712	02:04:08	+20:42:00		
	hsc727	02:08:20	+18:30:00		
	hsc746	02:15:20	+19:00:00		
	hsc755	02:17:32	+21:27:00		
	hsc774	02:22:32	+19:30:00		
	hsc786	02:26:08	+21:03:00		
	hsc804	02:32:08	+18:48:00		
	hsc808	02:33:20	+20:48:00		

Table 1 continued on next page

Table 1 *(continued)*

UT Date	Telescope	T	θ	Limit	Area
yyyy/mm/dd		(hrs)	(“)	(m_r)	(deg^2)
	hsc822	02:38:32	+15:33:00		
	hsc825	02:39:08	+19:12:00		
	hsc835	02:42:08	+21:09:00		
		.			
		.			
		.			
		.			
		.			

This is an abridged version, the full table and all the fields observed can be obtained at the Astronomical Journal or emailing the authors. The instruments used were HyperSuprimeCam on Subaru, DECam on CTIO4m, LB Camera on Large Binocular Telescope and IMACS on Magellan. These are fields in our survey in addition to the fields presented and detailed in Sheppard and Trujillo (2016). T is the approximate amount of time between the first and last images of a field, θ is the range of seeing for the night and Limit is the limiting magnitude in the r-band where we would have found at least 50% of the slow moving objects in most of the fields. Under the basic survey information for each night are the fields observed in J2000 coordinates for Right Ascension (hh:mm:ss) and Declination (dd:mm:ss). Field names were the names used at the telescope for each field and are likely to be unimportant, but are included for full information.

Table 2. Inner Oort Cloud and Extreme Trans-Neptunian Objects

Name	q (AU)	a (AU)	e	i (deg)	Ω (deg)	ω (deg)	$\bar{\omega}$ (deg)	b (deg)	Dist (AU)	Dia (km)	m_r (mag)
This Survey Inner Oort Cloud Discoveries											
2015 TG387	65 ± 1	1190 ± 70	0.945	11.669	300.97	118.2	59.2	10.7	80.0	300	24.0
2012 VP113	80.569	270.495	0.702	24.016	90.886	294.138	25.024	-16.637	82.873	450	23.22
Other Inner Oort Cloud Objects											
Sedna	76.167	540.623	0.859	11.928	144.502	311.106	95.608	-11.855	89.593	1000	21.04
This Survey Detached ETNOs Conservative Defintion ($q > 45$ au):											
2014 SR349	47.483	290.845	0.836	17.974	34.839	341.533	16.372	-17.1	57.2	200	24.1
This Survey Detached ETNOs Liberal Defintion ($q > 40$ au):											
2013 FT28	43.586	295.912	0.852	17.381	217.710	40.430	-101.860	-7.0	58.9	200	24.2

Above are the orbits of the Inner Oort Cloud Objects (IOCs) and Extreme Trans-Neptunian Objects (ETNOs) discovered in our survey. Quantities are the perihelion (q), semi-major axis (a), eccentricity (e), inclination (i), longitude of the ascending node (Ω), argument of perihelion (ω), longitude of perihelion ($\bar{\omega}$), ecliptic latitude at discovery (b), and distance at discovery (Dist). Diameter (Dia) estimates assume a moderate albedo of 0.15. Uncertainties for 2015 TG387, if not shown explicitly, are shown by the number of significant digits. Elements for Sedna and 2012 VP113 are taken from JPL Horizons and are truncated to 3 significant digits.

Table 3. Observational Bias Simulation Parameters

Parameter	Value	Description
		IOC Simulation Parameters
$R_{\rm min}$	50 au	Minimum heliocentric distance detectable in survey
$R_{\rm max}$	500 au	Maximum heliocentric distance detectable in survey
ρ	1000 kg m^{-3}	Density
p_r	0.15	Albedo in r filter
$r_{\rm min}$	20 km	Minimum radius
$r_{\rm max}$	1200 km	Maximum radius
$e_{\rm min}$	0.65	Minimum eccentricity
q'	4	Size distribution power law exponent
σ_i	6.9°	Sigma for Gaussian inclination distribution
μ_i	19.1°	Mean for Gaussian inclination distribution
a	2.7	Semi-major axis distribution power law exponent
$q_{\rm min}$	50 au	Minimum perihelion
$q_{\rm max}$	500 au	Maximum perihelion distance
$N_{\rm obs}$	2	Number of observed objects: 2012 VP113 and 2015 TG387
		Conservative ETNO + IOC simulation: same as IOC simulation except
$q_{\rm min}$	45 au	Minimum perihelion
$N_{\rm obs}$	3	Number of observed objects: 2012 VP113, 2015 TG387, 2014 SR349

Observational bias simulation parameters for both the IOC and ETNO+IOC combined simulation. We also ran simulations with both $q = 5$ and $a = 1$, as described in the text.

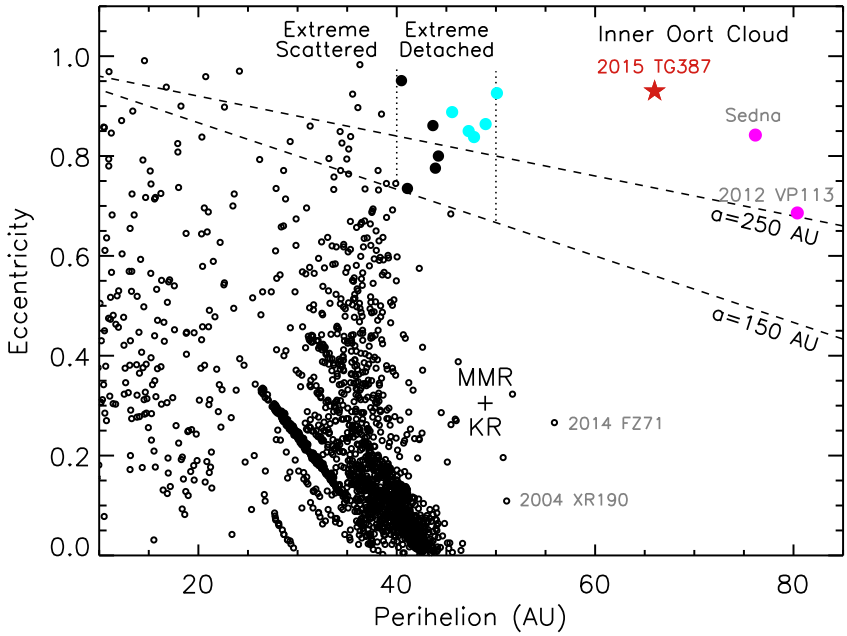

Figure 1. The perihelion versus eccentricity of small outer solar system objects with well known orbits as of July 2018 from the Minor Planet Center. The red star shows our new Inner Oort Cloud object 2015 TG387 with a perihelion near 65 au. Objects above the 150-250 au semi-major axis dashed lines are considered extreme. Bonafide Inner Oort Cloud objects are considered to have perihelion above 50 au (purple filled circles). Extreme detached objects are mostly decoupled from the giant planets and have perihelion between about 40-45 and 50 au (strictest definition with $45 < q < 50$ au and $a > 250$ au shown with filled blue circles, less extreme detached ETNOs shown with filled black circles). The less extreme detached ETNOs may have significant interactions with Neptune, while some may have a similar origin as the IOC objects. Extreme scattered disk objects have perihelia below 40 au and can have significant interactions with Neptune. Outer Oort cloud objects have aphelion above a few thousand au and can have significant interactions with outside forces such as the Galactic and stellar tides. Objects with relatively high perihelion beyond the Kuiper Belt edge at 50 au but only moderate eccentricity are likely created by a combination of past Neptune Mean Motion Resonances (MMR) and the Kozai Resonance (KR) and are detailed in Sheppard et al. (2016) and Kaib and Sheppard (2016). All object uncertainties are generally smaller than the symbols.

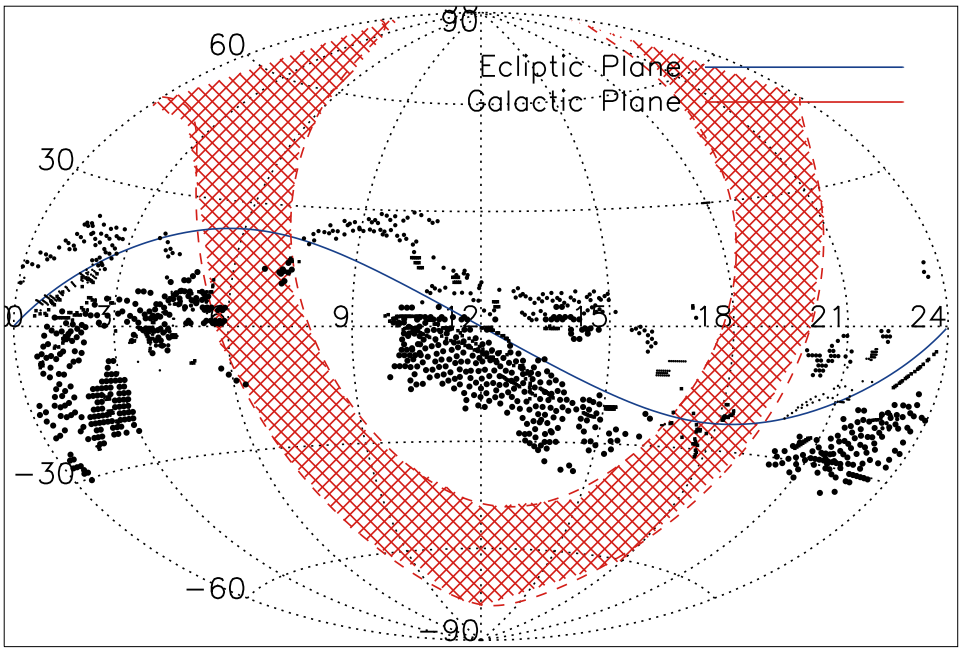

Figure 2. The newest survey fields were obtained using the HyperSuprime Camera on Subaru (medium circles) and the Dark Energy Camera on the CTIO 4m (large circles) as shown in Table 1. Also included in the figure are the fields detailed in Sheppard and Trujillo (2016). The Galactic plane is in red to ±15 degrees of the center. We covered about 1050 square degrees since Sheppard and Trujillo (2016), giving 2130 square degrees for the total survey to date.

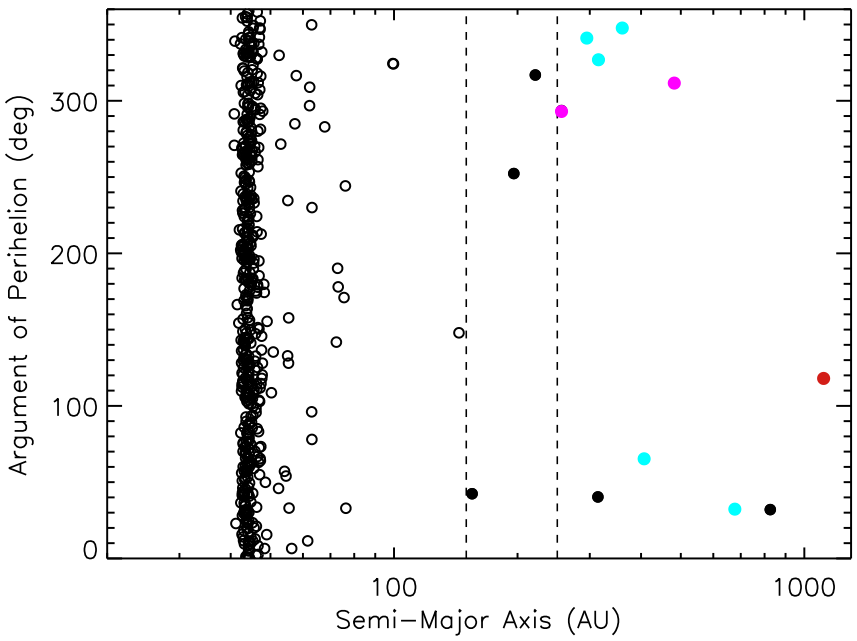

Figure 3. Semi-major axis versus argument of perihelion for all objects with perihelia greater than 40 au. Colors are the same as described in Figure 1. There is a noticeable clustering between 290 and 40 degrees, of which 2015 TG387 is the first detached extreme or inner Oort cloud object to be closer to 180 degrees than 0 degrees with a semi-major axis beyond 250 au.

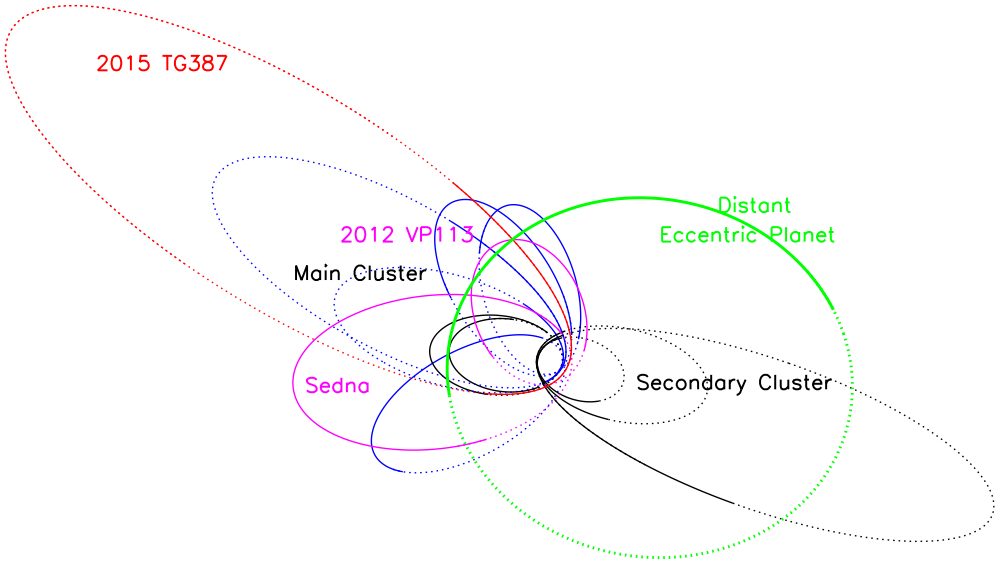

Figure 4. The plan view of the Inner Oort Cloud objects ($q > 50$ au: Sedna and 2012 VP113 in purple), detached ETNOs (most conservative definition in blue with $45 < q < 50$ au and $a > 250$ au: 2015 RX245, 2014 SR349, 2013 SY99, 2010 GB174, and 2004 VN112 and less conservative definition in black with $40 < q < 45$ au and $a > 150$ au: 2015 KG163, 2013 UT15, 2013 GP136, 2013 FT28, 2000 CR105) and the newly discovered IOC 2015 TG387 in red. All but the least conservative detached ETNOs are anti-aligned in longitude of perihelion with a possible distant planet on an eccentric orbit (in bold green). There is a second grouping of ETNOs that to date generally have lower perihelia and appear aligned with the planet in longitude of perihelion.

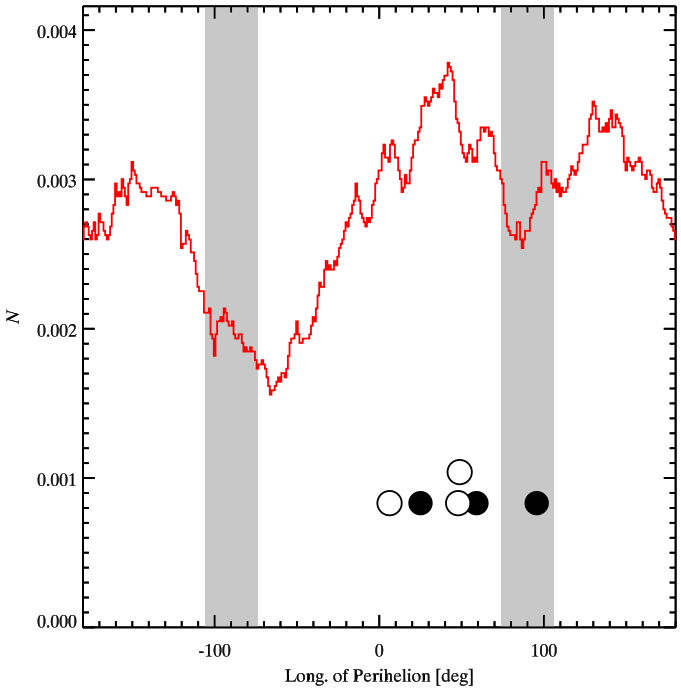

Figure 5. The normalized bias in longitude of perihelion in our survey fields for the IOC objects if drawn from a uniform longitude of perihelion distribution using the parameters shown in Table 3. The ecliptic longitudes within 15°of where the Galactic plane crosses the ecliptic are shaded in grey (southern declination is left and northern declination is right). The fact that the highest and lowest points differ by only about a factor 2 in all but a few cases suggests that our survey has fairly low observational biases for longitude of perihelion. The longitude of perihelion of Sedna, 2012 VP113 and 2015 TG387 are shown by solid circles while their location at discovery are shown by open circles.

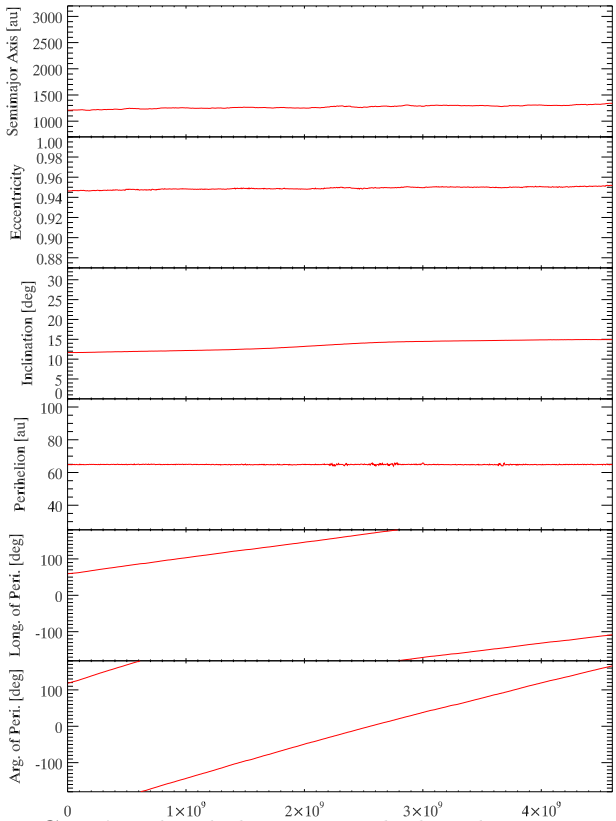

Figure 6. Evolution of 2015 TG387's orbital elements with the 4 known giant planets. The orbital elements for the nomial 2015 TG387 orbit is shown in red. Note that the longitude of perihelion and the argument of perihelion cycle through $\sim 360^\circ$ over the age of the solar system due to the action of the known major planets.

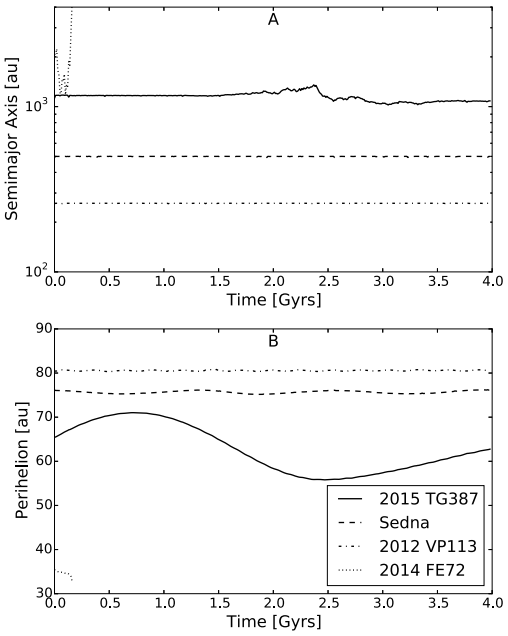

Figure 7. The behaviour of different extreme TNOs to the Galactic tide and 4 giant planets. 2015 TG387 is stable to the Galactic tide, though its perihelion now varies between about 55 and 70 au from Galactic tide interactions. Sedna, with a lower semi-major axis but aphelion still near 1000 au, has a slight variation in perihelion from the Galactic tide, while 2012 VP113, even more tightly bound, has almost no perihelion variation. 2014 FE72 has a larger semi-major axis and has its perihelion quickly driven down into the giant planet region by the Galactic tide and is lost. Notice how 2015 TG387's semi-major axis only starts to fluctuate when its perihelion is below about 60 au. This is from energy kicks from the giant planets.

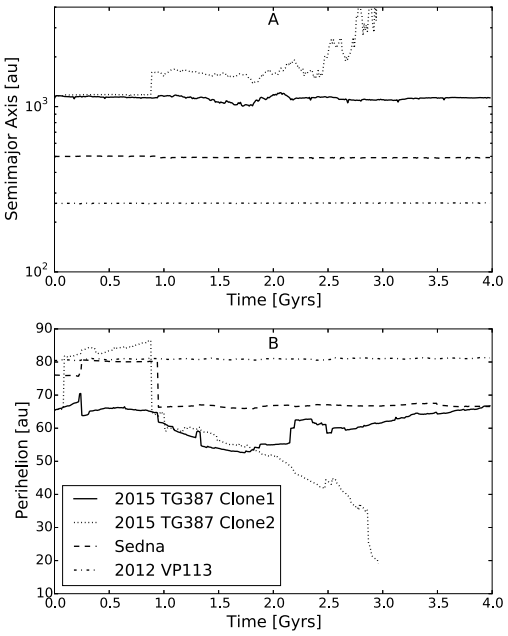

Figure 8. Same as Figure 7, but now also including stellar encounters. 2015 TG387 Clone 2, Sedna and 2012 VP113 are shown evolving in the strongest of our four stellar encounter simulations. Still 35% of 2015 TG387 clones survive the age of the solar system. Both Sedna and 2012 VP113 also have significant changes in their perihelia during the strongest stellar encounter simulation. In our other stellar encounter simulations some 99%, 95%, and 94% 2015 TG387 clones survive. 2015 TG387 Clone 1 has only small changes to its orbit over the age of the solar system in the moderate stellar encounter scenario that 95% of the 2015 TG387 clones survive. We find overall 2015 TG387 is likely stable to most stellar encounter scenarios over the age of the solar system.

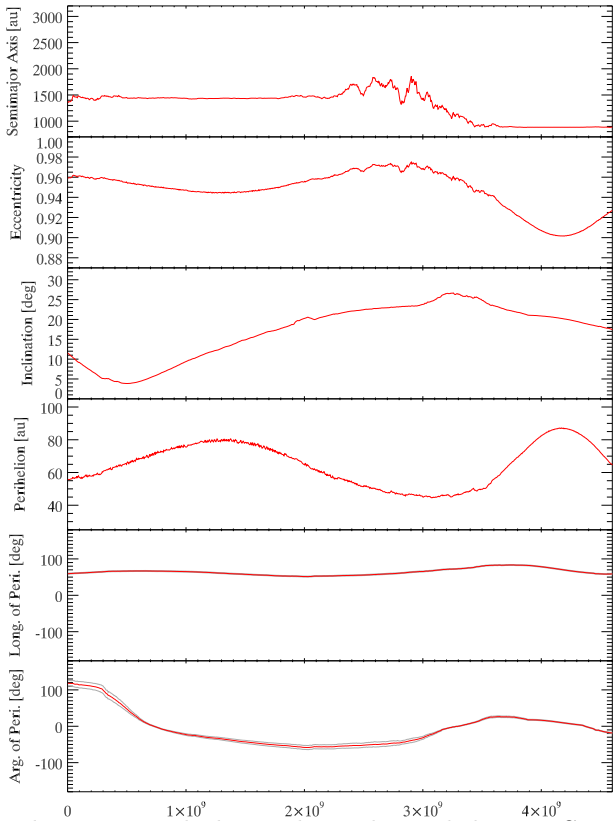

Figure 9. Same as Figure 6, but now including a hypothetical distant Super-Earth planet on an eccentric and inclined orbit beyond a few hundred Astronomical Units. A typical 2015 TG387 orbit is shown in red. In this simulation, the distant planet confines both the longitude of perihelion and the argument of perihelion of 2015 TG387, unlike without the planet in Figure 6. In particular, the longitude of perihelion of 2015 TG387 stays about 180 degrees away from, or anti-aligned with the planet for the age of the solar system. 2015 TG387's argument of perihelion also generally stays near 0 degrees after initially being much higher.

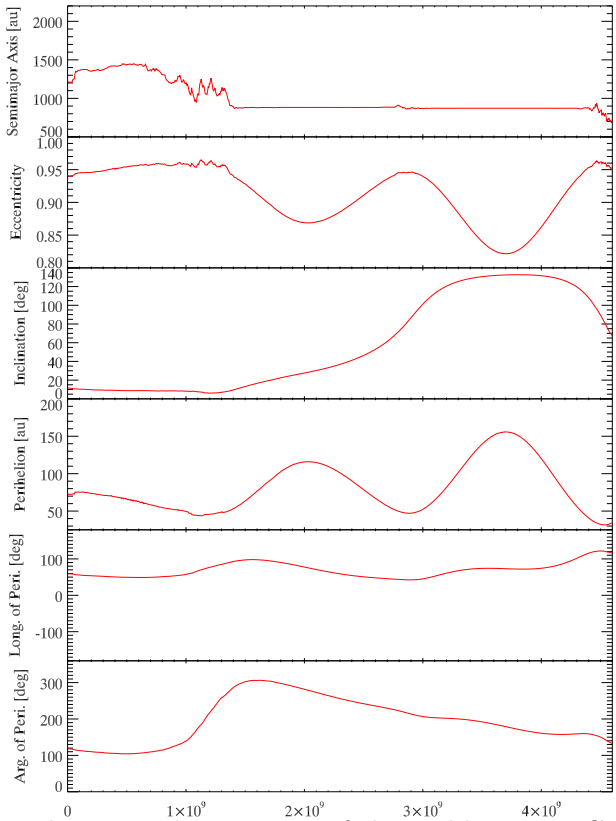

Figure 10. Same as Figure 9, but now showing one of the stable 2015 TG387 clones that went retrograde during the simulation. Retrograde 2015 TG387 clones occurred in all of the simulations that had stable ETNOs for the age of the solar system with a planet X. The longitude of perihelion is still constrained to remain anti-aligned with the planet for the age of the solar system.

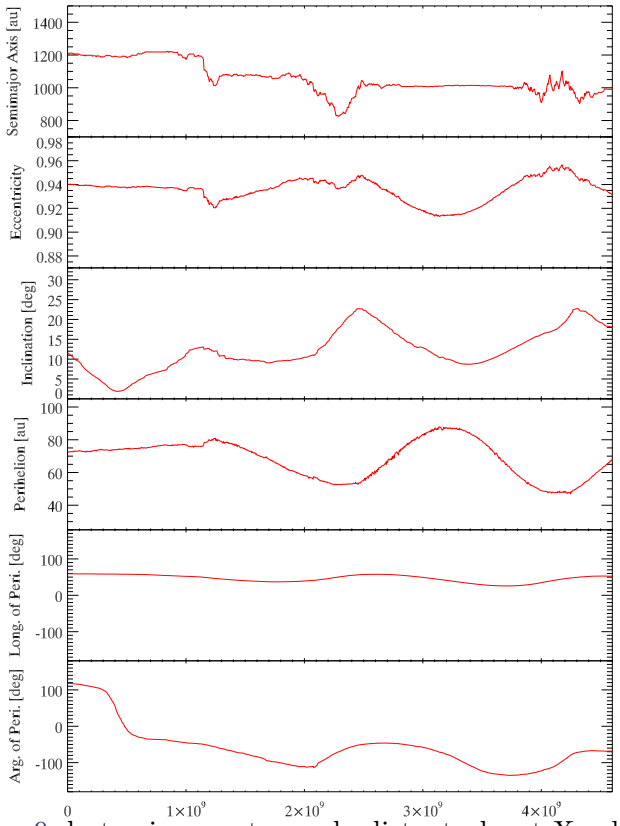

Figure 11. Same as Figure 9, but using a retrograde distant planet X orbit instead of a prograde orbit. All other aspects remain identical including clone choice and Planet X orbital elements not related to the change of Planet X from prograde to retrograde. As with the prograde case, the distant retrograde Planet X confines both the longitude of perihelion and the argument of perihelion of 2015 TG387. Other aspects of 2015 TG387's stability remain similar as well in both the prograde and retrograde Planet X scenarios.